PEROVSKITE $BiFeO_3$: EMERGING MATERIAL FOR WASTEWATER TREATMENT

Abstract

This chapter delves into the promising applications of $BiFeO_3$, a perovskite oxide, in the field of wastewater treatment. As global concerns regarding water pollution escalate, innovative solutions are imperative to address this critical issue. This chapter focuses on the unique properties and versatile characteristics of $BiFeO_3$ that position it as a novel contender for advanced wastewater treatment processes.

It begins by elucidating the fundamental properties of perovskite materials and their relevance to environmental remediation. It then delves into the synthesis methods and structural modifications of $BiFeO_3$ to enhance its performance in pollutant removal. The multifunctional nature of $BiFeO_3$, including its photocatalytic, adsorptive, and catalytic attributes, is explored in depth, shedding light on its efficacy in degrading a spectrum of organic pollutants, heavy metals, and even emerging contaminants.

Furthermore, it critically examines the factors influencing the photocatalytic efficiency and adsorption capacity of $BiFeO_3$, such as crystal structure, morphology, and surface area. Rare earth and transition metal substituted $BiFeO_3$ and the integration of $BiFeO_3$ into various hybrid nanocomposites and its synergistic effects for enhanced wastewater treatment are also discussed, highlighting the role of nanotechnology in advancing environmental remediation strategies.

Real-world applications and case studies showcase the successful utilization of $BiFeO_3$-based materials in treating wastewater from industrial, agricultural, and municipal sources. The material's scalability,

Authors

Sourabh Sharma
Materials Analysis and Research Laboratory
Department of Physics
Netaji Subhas University of Technology
Dwarka, New Delhi, India

Ashish
Department of Physics
Central University of Rajasthan
Ajmer, Rajasthan, India.

Ashok Kumar*
Nano Research Laboratory
Department of Physics
Deenbandhu Chhotu Ram University of Science and Technology
Murthal, Haryana, India
ashokkumar.phy@dcrustm.org

O. P. Thakur
Materials Analysis and Research Laboratory
Department of Physics
Netaji Subhas University of Technology
Dwarka, New Delhi, India

cost-effectiveness, and potential for regeneration contribute to its appeal as a sustainable solution for diverse wastewater treatment challenges.

In conclusion, "Perovskite $BiFeO_3$: Emerging Material for Wastewater Treatment" underscores the paradigm shift toward harnessing advanced materials like $BiFeO_3$ for tackling contemporary water pollution issues. Its comprehensive exploration of synthesis techniques, material properties, and application strategies provides valuable insights for researchers, engineers, and policymakers engaged in developing efficient and eco-friendly solutions to the global water crisis. As an emerging frontrunner in the realm of wastewater treatment, $BiFeO_3$ holds the promise of revolutionizing the way we approach water purification and environmental conservation.

Keywords: RE doped BFO, Photocatalysis, Adsorption Process, Dye degradation

I. INTRODUCTION

In the realm of advanced functional materials, the family of multiferroics has emerged as a captivating domain, drawing substantial interest due to their inherent ability to coalesce ferroelectric and magnetic characteristics within a single crystalline structure. Among these multifunctional materials, bismuth ferrite-based perovskites have emerged as remarkable entities that exhibit a harmonious interplay between ferroelectricity and magnetism, engendering unprecedented opportunities for an array of technological applications[1]. The pursuit of such materials is underscored by the pursuit of novel paradigms in electronics, spintronics, data storage, and sensor technologies, which capitalize on the synergy of multiple functionalities within a single lattice.

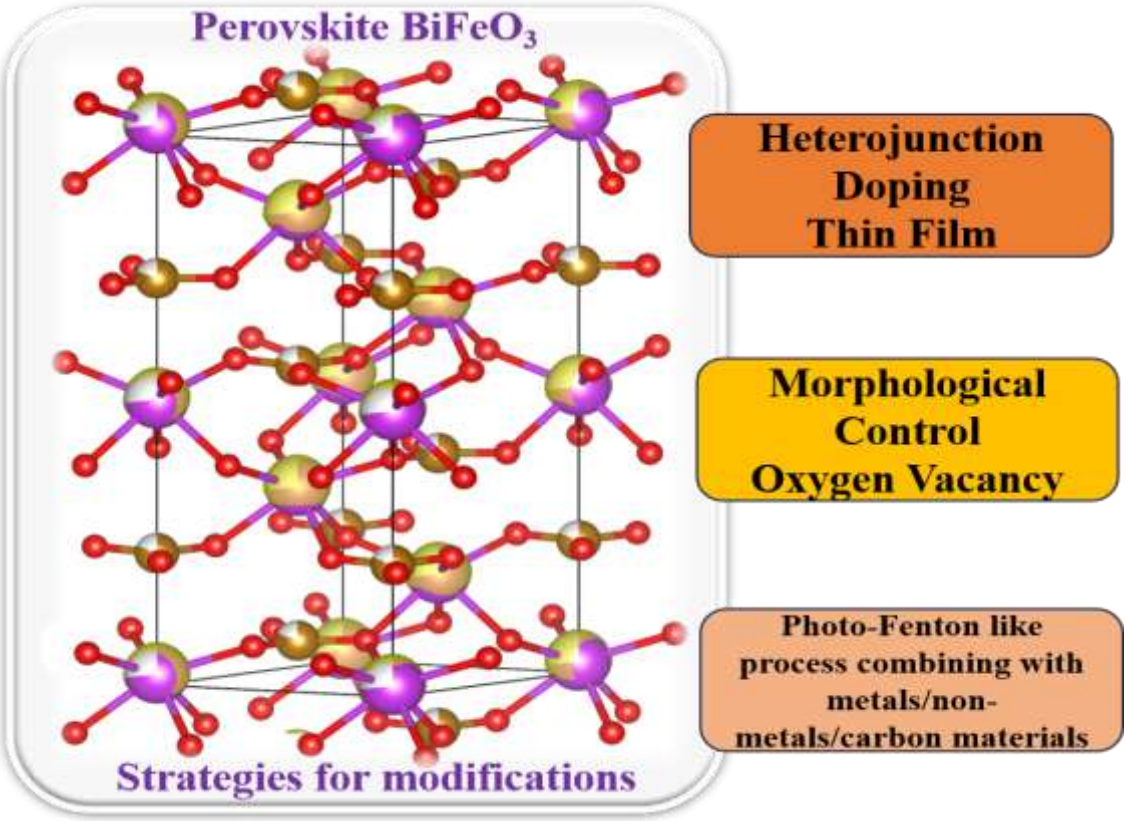

Bismuth ferrite ($BiFeO_3$), as the cornerstone of these perovskite multiferroics, evinces an intricate interweaving of its ferroelectric and magnetic properties. This arises from the elegant alignment of its crystal structure with the remarkable attributes of bismuth and iron ions. The displacement of bismuth ions from their ideal positions within the perovskite lattice engenders spontaneous polarization, resulting in pronounced ferroelectric behavior. Simultaneously, the iron ions, endowed with their magnetic moments, contribute to the manifestation of magnetic order, resulting in a rare coexistence of ferroelectricity and magnetism that is deeply intertwined[2]. The emergence of bismuth ferrite-based perovskites as multifunctional materials is a consequence of their unique crystal structure, which adheres to the ABX_3 perovskite prototype. Here, the B-site is occupied by the iron ions (Fe^{3+}), while the A-site is inhabited by bismuth ions (Bi^{3+}), creating a symphony of charge imbalances that underpins the material's multiferroic attributes. The resulting structural configuration is the crucible in which the material's distinctive properties gestate, setting the

stage for its diverse technological manifestations[3].The synthesis of bismuth ferrite-based perovskites, a pivotal aspect of their exploration, is pivotal in tailoring their properties for specific applications. An array of synthesis methods has been devised, including the venerable solid-state reaction, the versatile sol-gel process, the nuanced hydrothermal synthesis, and the precise chemical vapor deposition[4]. Each approach engenders a distinct interplay of temperature, pressure, precursor composition, and reaction kinetics, imparting unique morphological and compositional features upon the resultant material. This multidisciplinary exploration necessitates comprehensive characterization techniques to unveil the materials' intricate attributes. Advanced methodologies such as X-ray diffraction (XRD) elucidate the crystallographic structure and phase purity, while electron microscopy techniques, including scanning electron microscopy (SEM) and transmission electron microscopy (TEM), unravel morphological features at diverse length scales. Complementary techniques like Fourier-transform infrared spectroscopy (FTIR) delve into vibrational modes and intermolecular interactions, providing insights into chemical bonding and surface modifications[5].

The fundamental premise underpinning their multifunctionality resides in the unique attributes of bismuth and iron ions encapsulated within the ABX_3 perovskite lattice. Bismuth ferrite ($BiFeO_3$), a linchpin of this genre, exhibits ferroelectric polarization arising from the displacement of bismuth ions, coupled with magnetic order bestowed by iron ions[6].

BFO nanostructures are particularly interesting due to their excellent properties, attributed to their large surface areas and diverse morphologies[7].

1. **BFO Ceramics ($BiFeO_3$ Ceramics):**

- Synthesized first in 1957, BFO ceramics are crucial nanomaterials.
- Challenges during synthesis include volatility of Bi^{3+} and the formation of oxygen vacancies, leading to secondary phases and current leakage.
- Strategies like ion substitution and alloying with ABO_3 compounds are employed to enhance physical behavior.

2. **BFO Thin Films ($BiFeO_3$ Thin Films):**

- Easier fabrication compared to ceramics, attracting recent attention.
- Epitaxial BFO film structure depends on thickness and strain on different substrates.
- Doping or forming solid solutions can influence the film's structure.

3. **BFO Nanostructures ($BiFeO_3$ Nanostructures):**

- Considered a research hotspot for unique photocatalytic and magnetic properties.
- Various morphologies include nanodots, nanofibers, nanosheets, nanoplates, nanotubes, nano islands, nanoparticles, microplates, and nanowires.
- Particle size influences magnetic response, and larger particles exhibit enhanced magnetization.
- BFO nanofibers prepared using electrospinning and sol–gel chemistry showed excellent photoactivity against rhodamine-B dye under both UV and visible light with H_2O_2.

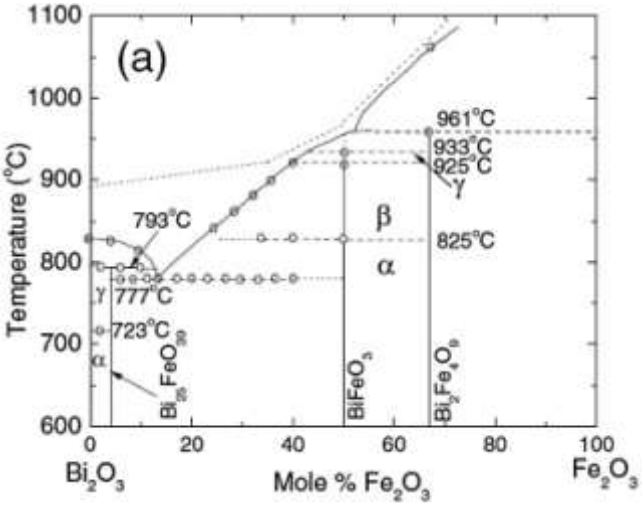

Figure 1: Phase diagram of BFO[8] (Licence No. RNP/24/FEB/075034)

BFO nanostructures are notable for their distinctive properties, offering potential applications in photocatalysis and magnetism. The synthesis of BFO ceramics faces challenges, prompting the use of strategies like ion substitution and alloying to improve their physical behavior[5]. BFO thin films, being easier to fabricate, have gained recent attention, with their structure influenced by thickness, substrate, and doping.

II. SYNTHESIS METHODOLOGIES

1. **Solid-State Reaction:** The venerable solid-state reaction method stands as an emblem of simplicity and cost-effectiveness in synthesizing bismuth ferrite-based perovskites. In this methodology, high-purity powders of bismuth oxide ($Bi_2 O_3$) and iron oxide ($Fe_2 O_3$) are meticulously combined in stoichiometric ratios, followed by thermal calcination at elevated temperatures[9]. While its simplicity is commendable, the solid-state reaction method often struggles to yield high purity due to the formation of intermediate phases. Additionally, prolonged annealing can foster grain growth, affecting the resulting material's grain size and homogeneity.

2. **Sol-Gel Process:** The sol-gel process emerges as a versatile contender, conferring meticulous control over the material's properties. By hydrolyzing metal alkoxides or nitrates, a precursor solution is crafted. This solution subsequently undergoes gelation and thermal treatment to yield the desired perovskite phase[10]. The sol-gel approach facilitates the incorporation of dopants, manipulation of particle size and morphology, and the fabrication of thin films. However, organic residuals from the precursors can lead to defects, and achieving high-density ceramics can pose challenges.

3. **Hydrothermal Synthesis:** Hydrothermal synthesis, a favoured methodology for producing nanoscale bismuth ferrite-based perovskites, capitalizes on high-pressure and high-temperature aqueous conditions. Precursor solutions undergo chemical reactions under these conditions, culminating in the formation of nanoparticles[11]. This approach bestows control over particle size, crystallinity, and morphology, presenting a gateway to tailored nanoscale structures. However, the necessity for specialized equipment and the potential for vessel-induced contamination warrants careful consideration.

4. **Chemical Vapor Deposition (CVD):** Chemical vapor deposition presents a pathway to precision, specifically in growing thin films on substrates. Volatile precursor compounds are introduced into a reaction chamber and thermally decomposed, depositing a thin film on the substrate's surface. This technique bestows control over film thickness, composition, and uniformity, catering to integrated electronic and photonic applications[12]. Nevertheless, the challenge lies in achieving uniform decomposition and film coverage, especially on complex substrates.

Perovskite-type oxides are commonly synthesized through solid-state reactions involving oxide precursors subjected to elevated temperatures. For instance, $BiFeO_3$ (BFO) has traditionally been synthesized using equal portions of Bi_2O_3 and Fe_2O_3. The phase diagram depicting the Bi_2O_3–Fe_2O_3 system reveals that BFO is an incongruently melting compound. Consequently, during the phase formation kinetics within this system, impurities such as $Bi_2Fe_4O_9$, Bi_2O_3, or $Bi_{25}FeO_{40}$ may emerge[13]. Consequently, conventional solid-state reaction pathways for BFO preparation may inadvertently yield these impurity phases due to BFO's limited stability at high temperatures.

III. DOPING APPROACHES

1. **Cationic Doping:** Cationic doping involves the substitution of bismuth (Bi^{3+}) and iron (Fe^{3+}) ions with other cations, imparting a subtle yet profound impact on material properties. Rare-earth cations like lanthanum (La^{3+}) or yttrium (Y^{3+}) have been introduced to manipulate lattice parameters, induce strain, and modulate polarization states. Such dopants may influence the ferroelectric polarization by altering the crystal symmetry, ultimately affecting the multiferroic coupling[14]. Furthermore, transition metal ions such as cobalt (Co^{3+}) or manganese (Mn^{2+}) can engender altered magnetic moments, impacting magnetic ordering and leading to modified multiferroic responses.

2. **Anionic Doping:** Anionic doping involves the introduction of foreign anions, such as oxygen vacancies or fluorine ions, into the perovskite lattice. Oxygen vacancies can lead to charge imbalances, affecting ferroelectric polarization and band structure. Fluorine doping, on the other hand, can modify electronic properties by altering the charge distribution around the metal ions[15]. These anionic dopants influence defect chemistry, altering the balance between ferroelectric and magnetic domains and potentially fostering enhanced multiferroic coupling.

3. **Dual-Ion Dopants:** Dual-ion doping strategies involve the simultaneous incorporation of cations and anions to engineer complex defect structures. For example, bismuth ferrite-based perovskites doped with lanthanum (La^{3+}) and titanium (Ti^{4+}) exhibit enhanced ferroelectric and piezoelectric responses due to the coupling of cationic and anionic defects[16]. Such dual-doping strategies leverage the synergy between cationic and anionic dopants to create tailored energy landscapes, impacting ferroelectric and magnetic transitions in.

4. **Nonstoichiometric Dopants:** The introduction of nonstoichiometric dopants, such as vacancies or interstitials, offers a nuanced approach to doping. Oxygen vacancy doping, for instance, introduces electron traps that can influence charge carrier dynamics, thus altering ferroelectric and magnetic responses. The deliberate introduction of oxygen

vacancies or other nonstoichiometric defects can induce phase transitions or modify crystal symmetry, thereby influencing multiferroic behavior.

5. **Implications for Multiferroic Behavior:** Doping strategies in bismuth ferrite-based perovskites have far-reaching implications for multiferroic behavior. By judiciously selecting dopants and tailoring their concentrations, researchers can control the balance between ferroelectric and magnetic orders. This delicate equilibrium directly influences the coupling between electric and magnetic domains, a cornerstone of multiferroic behavior[17]. Doping-induced strain, defect chemistry, and altered electronic configurations orchestrate the synergy between ferroelectric polarization and magnetic ordering, thereby influencing the material's overall multiferroic response.

Bismuth ferrite-based perovskites have gained prominence as an intriguing class of materials due to their simultaneous ferroelectric and magnetic characteristics, emblematic of multiferroic behavior. These attributes emerge from the unique arrangement of bismuth and iron ions within the perovskite lattice. Doping, the deliberate introduction of foreign ions, offers a powerful avenue to tailor the properties of these materials. This article delves into the distinct impacts of A-site and B-site doping on bismuth ferrite-based perovskites, elucidating their consequences for the interplay between ferroelectric and magnetic domains.

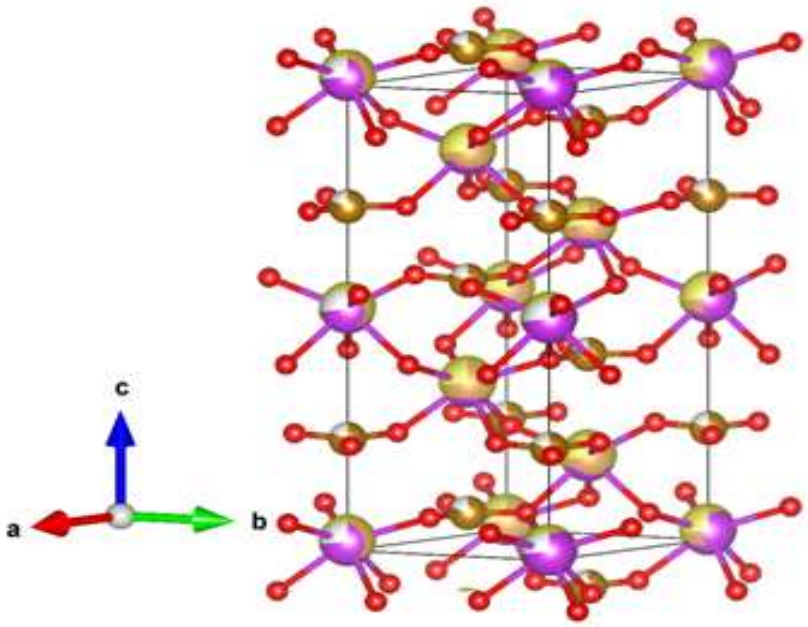

Figure 2: ABO_3 orthorhombic perovskite structure unit cell schematic presentation

- **A-site Doping:** A-site doping involves the substitution of bismuth ions (Bi^{3+}) with foreign cations, often altering the overall charge balance and lattice symmetry. This doping strategy has a pronounced influence on the crystallographic structure and the resulting electronic and vibrational properties. For instance, rare-earth ions such as lanthanum (La^{3+}) can replace bismuth in the A-site, inducing strain and modifying polarization states. A-site doping can lead to changes in the lattice parameters, impacting the ferroelectric Curie temperature and influencing the overall ferroelectric

response. Moreover, the introduction of larger cations can create local lattice distortions, fostering a more intricate coupling between ferroelectric and magnetic orders[18].

In 2019, a study on nanoparticles of $Bi_{1-x}Ba_xFeO_3$ (x = 0–0.20), was synthesized using a molten solid-state method. They found that all the nanoparticles crystallized in a rhombohedral structure with the space group R3c. With increasing Ba doping, particle sizes decreased, and particle shapes changed from cubic or rectangular to spherical, as observed in SEM images. The introduction of Ba led to enhanced magnetization in the nanoparticles (BBFO) due to disruptions in the original spiral spin structure. The study also revealed that Ba doping decreased leakage current densities by about an order of magnitude due to impurity phase and oxygen vacancy suppression. This doping also improved dielectric properties[19]. The remanent magnetization of BBFO nanoparticles was measured at 0.51 emu/g, and their leakage current density was remarkably low at 1.15 nA/cm^2, contrasting with the 10.1 nA/cm^2 found in undoped BFO nanoparticles.

Additionally, the dielectric properties of the nanoparticles were influenced by their particle sizes. Smaller grain sizes in Ba-doped BFO nanoparticles resulted in lower dielectric constants due to particle size effects. The study reported enhanced ferroelectric properties such as increased remnant polarization (Pr) and reduced leakage current density due to structural distortion caused by Ba doping. The reduction in dielectric loss as Ba content increased was attributed to the mitigation of oxygen vacancies through Ba doping. The remnant polarization value showed an initial increase followed by a decrease due to charge fluctuation between Fe^{3+} and Fe^{2+} ions[20].

Lead (Pb) holds significant importance in energy storage applications, particularly in batteries, due to its capacity for high-charge storage and short bursts of high current. This attribute makes lead pivotal in enhancing supercapacitor efficiency. Mazumder and Sen reported Pb-doped $BiFeO_3$ ($Bi_{1-x}Pb_xFeO_3$, x=0.03–0.07) powders with distinct properties. Dielectric constant and dissipation factor decreased with frequency increase. The dielectric constant decrease in Pb-doped $BiFeO_3$ was attributed to augmented space-charge polarization. Pb addition elevated electrical resistivity, leading to non-lossy ferroelectric hysteresis loops in $BiFeO_3$ ceramics.

Pb-doped $La_{0.1}Bi_{0.9-x}Pb_xFeO_3$ samples, prepared using a sol–gel auto-ignition technique, were studied systematically. Pb doping resulted in larger, more porous grains. La doping shifted BFO's structure from rhombohedral to pseudo-tetragonal, while Pb doping induced a pseudo-cubic structure. Dielectric constant reduced with Pb doping, influenced by combined dielectric relaxation involving oriental polarization and charge carrier conduction. Similar dielectric trends emerged in Mn-doped, Sr-doped, Sm-doped, Pr-doped, and Dy-doped BFO materials. Dielectric parameters slightly increased with rising temperature due to thermally induced hopping conduction enhancement. The structural transformation from rhombohedral to pseudo-cubic was extensive and disrupted spatial spin structure, resulting in substantial latent magnetization compared to other samples. In summary, Pb doping in $BiFeO_3$-based materials induced diverse structural changes and influenced dielectric properties, contributing to advancements in energy storage technology[21].

- **B-site Doping:** B-site doping involves the substitution of iron ions (Fe^{3+}) with foreign cations, leading to alterations in magnetic moments and spin configurations. This doping approach holds the potential to modulate the magnetic ordering and spin coupling within the material. Transition metal ions, such as manganese (Mn^{3+}) or cobalt (Co^{3+}), can be introduced to manipulate the magnetic behavior. B-site doping can induce modifications in the spin exchange interactions, leading to shifts in magnetic transition temperatures and potentially affecting the multiferroic coupling. Such dopants can impart a substantial influence on the overall magnetic and ferroelectric behavior of the material[22].

Research has focused on enhancing the multiferroic attributes of $BiFeO_3$ (BFO) by reducing its size to the nanoscale and improving its magnetic properties through cation substitution via B-site (Fe-site) doping, often using magnetic ions like Ni. This substitution aims to enhance magnetization and is based on the similarity in ion radius between Ni and Fe, benefiting from the size effect of nanostructures on magnetic properties.

Nadeem et al. synthesized BFO and Ni-doped BFO nanoparticles via the low-temperature sol-gel method. The remanent polarization of Ni-doped BFO was significantly higher (19.43 times) than that of pure BFO. Ni doping led to substantial improvements in the dielectric, magnetic, and ferroelectric properties of BFO. This enhancement in magnetization might be attributed to the suppression of the spin spiral structure due to nanoscale particles. Dielectric constant and loss tangent decreased with increasing frequency, likely due to interfacial/space-charge polarization. The dielectric constant's strength correlated with space charge and oxygen vacancy density[23]. Ni doping also led to a decrease in leakage current by suppressing impurity phases, effectively enhancing BFO's dielectric and multiferroic properties, and potentially benefiting various device applications.

Betancourt-Cantera et al. synthesized $BiFe_{1-x}Ni_xO_3$ ($0 \leq x \leq 0.5$) through high-energy ball-milling, investigating structural and multiferroic characteristics. Their study explored modifications in electrical conductivity, permittivity, and dielectric loss across frequencies, linked to crystal structure changes with varying nickel concentrations. The presence of nickel caused an increase in dielectric loss and conductivity due to generated oxygen vacancies.

Manganese (Mn) substitutions in BFO have been recognized for their ability to enhance both ferromagnetic and ferroelectric characteristics. This enhancement arises from their potential presence in Mn^{3+} and Mn^{4+} valence states, crucially affecting domain wall dynamics in multiferroic materials. Ghahfarokhi et al. conducted a study on Mn-doped BFO nanoparticles prepared via the sol-gel method, revealing a decrease in crystallite size as doping concentration increased. The nanoparticles exhibited robust ferromagnetic properties and increased bandgap with higher doping levels. Doping led to decreased dielectric constant and dielectric loss, while electrical conductivity increased.

Dhanalakshmi et al. synthesized multiferroic Mn-doped BFO nanoparticles using the sol-gel auto-combustion method. Manganese's multivalent states contributed

to reduced oxygen vacancies, subsequently impacting electrical and magnetic properties[24]. This study indicated an improvement in dielectric and ferromagnetic properties, accompanied by enhanced magnetoelectric coupling. The increased Mn concentration correlated with a relatively high dielectric constant (ε'), affirming space-charge polarization.

The presence of mixed valence states of Fe ions (Fe^{2+}/Fe^{3+}), oxygen vacancies, and the spiral spin modulation in BFO systems pose challenges in achieving net magnetization and ferromagnetism. To address these issues, Ti doping has emerged as an effective approach. Ti^{4+} ions can mitigate the concentrations of oxygen vacancies and Fe^{2+} ions in BFO ceramics, leading to reduced dielectric loss and conductivity. This doping method also boosts magnetization by disrupting the equilibrium between adjacent antiparallel spin lattices of Fe^{3+} ions.

Research by Tian et al. showcased the effectiveness of Ti-doped BFO nanoceramics in controlled polarization switching through electric fields, thus manipulating ferroelectric domains at the nanoscale. Ti doping led to the observation of substantial remanent polarization (P_r) and maximum polarization (P_{max}) values, surpassing those found in pure BFO ceramics. In essence, Ti doping has proven to be a promising strategy for addressing challenges related to polarization control, dielectric properties, and magnetization enhancement in BFO systems.

Lead (Pb) holds significant importance in energy storage applications, particularly in batteries, due to its capacity for high-charge storage and short bursts of high current. This attribute makes lead pivotal in enhancing supercapacitor efficiency. Mazumder and Sen reported Pb-doped $BiFeO_3$ ($Bi_{1-x}Pb_xFeO_3$, x=0.03–0.07) powders with distinct properties. Dielectric constant and dissipation factor decreased with frequency increase. The dielectric constant decrease in Pb-doped $BiFeO_3$ was attributed to augmented space-charge polarization. Pb addition elevated electrical resistivity, leading to non-lossy ferroelectric hysteresis loops in $BiFeO_3$ ceramics.

Pb-doped $La_{0.1}Bi_{0.9-x}Pb_xFeO_3$ samples, prepared using a sol–gel auto-ignition technique, were studied systematically. Pb doping resulted in larger, more porous grains. La doping shifted BFO's structure from rhombohedral to pseudo-tetragonal, while Pb doping induced a pseudo-cubic structure. Dielectric constant reduced with Pb doping, influenced by combined dielectric relaxation involving oriental polarization and charge carrier conduction. Similar dielectric trends emerged in Mn-doped, Sr-doped, Sm-doped, Pr-doped, and Dy-doped BFO materials. Dielectric parameters slightly increased with rising temperature due to thermally induced hopping conduction enhancement. The structural transformation from rhombohedral to pseudo-cubic was extensive and disrupted spatial spin structure, resulting in substantial latent magnetization compared to other samples. In summary, Pb doping in BiFeO3-based materials induced diverse structural changes and influenced dielectric properties, contributing to advancements in energy storage technology[25].

6. **Rare Earth Metal Doping:** Rare-earth elements, known for their distinctive magnetic, electrical, and spectroscopic attributes, significantly enhance energy conversion processes. In a study by Rhaman et al. in 2019, pure and Sm-doped BFO particles were synthesized using the sol-gel method. Substituting Sm into BFO induced a transformation

from rhombohedral to orthorhombic structure, accompanied by reduced crystallite size. Increasing Sm concentration led to higher dielectric constants that diminished with frequency rise. Enhanced dopant concentration reduced dielectric loss, attributed to increased structural stability and fewer impurity phases[26]. The rise in dopant concentration also elevated maximum polarization, decreasing leakage current density through impurity phase suppression. At low frequencies, doped samples exhibited notably decreased electrical resistance, reactance, and resistivity, remaining relatively constant at high frequencies.

A separate study in 2016 by Awan et al. successfully synthesized La-doped $BiFeO_3$ (BLFO) nanoparticles via a nonvacuum sol-gel technique. At a 0.3 wt% dopant concentration, the resulting nanoparticles displayed robust ferromagnetic behavior. The emergence of ferromagnetism in $BiFeO_3$ was attributed to the linearity in the spin structure. These findings suggest the potential of Sm-doped BFO for applications in memory devices, PV solar cells, and energy storage. In a similar vein, La-doped $BiFeO_3$ nanoparticles demonstrated strong ferromagnetic properties at a specific dopant concentration, as reported by Awan et al. in 2016.

Oxygen vacancy formation is a well-recognized phenomenon in BFO, occurring through the loss of oxygen. These vacancies occur both within the bulk and at the surface, influencing O-site substitutions. The introduction of oxygen vacancies induces alterations in both the electrical and magnetic characteristics of BFO[27]. Seidel et al. conducted a study on $B_{0.9}Ca_{0.1}FeO_{3–0.05}$, revealing the influence of oxygen vacancies on its electrochemical properties.

7. **Doping with Carbon Materials:** In environmental cleanup applications, carbon materials are promising due to their corrosion resistance, thermal stability, large surface area, and good electronic properties. Combining carbon materials with semiconductor materials, like Bismuth Ferrite (BFO), can enhance their photocatalytic performance. Previous studies have shown that such combinations can reduce electron-hole recombination and increase pollutant adsorption on the composite material.

For example, in a study by Li et al., BFO-graphene (BG) composites were synthesized using a hydrothermal method. The coupling of BFO nanoparticles and graphene was improved by creating Fe-O-C bonds through the adsorption of OH groups on the graphene surface. This enhanced coupling was confirmed by Raman analysis. The resulting composites showed better photocatalytic performance for degrading Congo Red (CR) compared to BFO and graphene mixtures or BFO alone under visible light[28]. The improved performance was attributed to the modified band gap and covalent bonding between BFO and graphene. Due to the large graphene p-conjugation plane, CR could strongly adsorb on the graphene surface, shifting its absorption spectra.

In another study by Wang et al., BFO spindle-like nanoparticles were decorated on graphitic carbon nitride (g-C_3N_4) nanosheets using a simple deposition-precipitation method. The resulting BFO/g-C_3N_4 nanocomposites exhibited significantly higher photodegradation efficiency (around 75%) for degrading methyl orange (MO) under visible light compared to pristine g-C_3N_4 and BFO alone.

8. **Interplay and Multiferroic Implications:** The interplay between A-site and B-site doping is a dynamic interplay that influences the delicate balance between ferroelectric and magnetic orders. Altering the A-site cations can perturb the crystal symmetry, impacting the ferroelectric response and, consequently, the multiferroic behavior. This, in turn, can affect the magnetic order and spin configurations through spin-lattice coupling. Simultaneously, by modifying the magnetic interactions, B-site doping can modulate the ferroelectric polarization through spin-driven mechanisms.

   The strategic combination of A-site and B-site doping can yield synergistic effects, leading to enhanced multiferroic properties. By carefully selecting dopants for both sites, researchers can harness the interplay between charge, lattice, and spin degrees of freedom to amplify the coupling between ferroelectric and magnetic domains. This coupling holds the key to unlocking advanced functionalities, such as electric field control of magnetization or magnetoelectric effects, with far-reaching implications for multifunctional devices and applications.

   Since 2007, the extensive research on BFO has primarily centered around its exceptional photoactivity. It has demonstrated noteworthy efficiency in degrading common organic pollutants, particularly in aqueous environments[29]. Various model contaminants like methylene blue (MB), rhodamine B (RhB), methyl orange (MO), 4-chlorophenol, and 4-nitrophenol have been utilized in these reactions. However, there remains a dearth of literature addressing gaseous phase reactions. These photocatalytic processes involve a multitude of experimental factors, including nanostructure, surface area, photocatalyst loading, organic pollutant type, initial pollutant concentration, and light source. Consequently, direct comparisons between different laboratories' photocatalytic experiments are intricate. Nonetheless, a comprehensive understanding can be cultivated by delving into photoactivity and degradation mechanisms, as elaborated below.

9. **Photocatalytic Degradation:** The photocatalytic degradation efficiency of Bismuth Ferrite ($BiFeO_3$) based perovskite multiferroics depends on a variety of factors, including the material's structural properties, electronic band structure, surface area, and the nature of the target pollutants. While $BiFeO_3$ itself possesses some photocatalytic activity due to its intrinsic multiferroic behavior, its efficiency can be enhanced through various strategies[30]. Below, I'll provide an overview of how these factors influence the photocatalytic degradation efficiency of $BiFeO_3$ -based perovskite multiferroics:

   - **Band Gap and Electronic Properties:** The band gap of the material plays a crucial role in determining its photocatalytic activity. $BiFeO_3$ has a relatively wide band gap (~2.2 eV), which limits its photocatalytic efficiency in the visible light region. To enhance its efficiency, band gap engineering can be employed. This can be achieved through doping with transition metals or other elements to modify the electronic band structure, thereby allowing the absorption of a broader range of visible light.

   - **Surface Area and Morphology:** The surface area and morphology of the photocatalyst significantly impact its photocatalytic performance. Nanostructuring $BiFeO_3$ into nanoparticles, nanorods, or thin films can increase its surface area,

facilitating greater interaction with pollutants. Higher surface area enables more active sites for photocatalytic reactions, leading to improved degradation efficiency.

- **Ferroelectric Polarization:** The inherent ferroelectric polarization in $BiFeO_3$ can contribute to its photocatalytic activity. Polarization-induced charge separation at the surface can enhance electron-hole separation, reducing recombination rates and thereby enhancing the efficiency of photocatalytic reactions.

- **Heterojunctions and Co-catalysts:** Creating heterojunctions or coupling $BiFeO_3$ with other semiconductor materials can enhance photocatalytic activity. These heterojunctions can facilitate efficient charge transfer and separation[31]. Additionally, co-catalysts like noble metals or metal oxides can promote electron-hole separation and improve overall degradation efficiency.

- **Visible Light Absorption:** Since $BiFeO_3$'s band gap is in the UV range, enhancing its visible light absorption is crucial. Strategies like elemental doping (e.g., nitrogen or carbon) or sensitization with organic dyes can extend the absorption range to visible light, thereby increasing the utilization of solar energy.

- **Photogenerated Reactive Species:** In photocatalysis, photogenerated reactive species like hydroxyl radicals (•OH) and superoxide radicals (O_2 $^{\bullet -}$) are responsible for pollutant degradation. Enhancing the production and lifetime of these species through improved charge separation and efficient utilization of photogenerated electrons and holes is crucial for higher degradation efficiency.

- **Target Pollutants and Reaction Conditions:** The efficiency of $BiFeO_3$-based photocatalysis can vary based on the nature of the target pollutants. The pH, temperature, and the presence of electron donors or scavengers can significantly influence the photocatalytic degradation process.

In conclusion, while Bismuth Ferrite ($BiFeO_3$) itself has inherent photocatalytic activity due to its multiferroic nature, its efficiency can be significantly enhanced by band gap engineering, morphology optimization, heterojunction formation, co-catalyst introduction, and other strategies. These modifications aim to improve visible light absorption, charge separation, and utilization of photogenerated reactive species, ultimately leading to higher photocatalytic degradation efficiency of pollutants[32].

REFERENCES

[1] M. Kumar, P. C. Sati, S. Chhoker, and V. Sajal, Ceram. Int. 41, 777 (2015).
[2] G. Catalan and J. F. Scott, Adv. Mater. 21, 2463 (2009).
[3] W. Eerenstein, N. D. Mathur, and J. F. Scott, Nature 442, 759 (2006).
[4] D. L. Golić, A. Radojković, A. Dapčević, D. Pajić, J. Dragović, F. Torić, J. Ćirković, G. Branković, and Z. Branković, Ceram. Int. 45, 19158 (2019).
[5] N. Sheoran, A. Kumar, V. Kumar, and A. Banerjee, J. Supercond. Nov. Magn. 33, 2017 (2020).
[6] V. Verma, J. Alloys Compd. 641, 205 (2015).
[7] A. K. Sahu, P. Mallick, S. K. Satpathy, and B. Behera, Adv. Mater. Lett. 12, 1 (2021).
[8] R. Palai, R. S. Katiyar, H. Schmid, P. Tissot, S. J. Clark, J. Robertson, ... and J. F. Scott, Phys. Rev. B, 77(1), 014110 (2008).

[9] S. Chauhan, C. Anand, B. Tripathi, M. Kumar, M. Sahni, R. C. Singh, and S. Singh, J. Mater. Sci. Mater. Electron. 31, 20191 (2020).
[10] R. Das, T. Sarkar, and K. Mandal, J. Phys. D. Appl. Phys. 45, (2012).
[11] T. Sahu and B. Behera, Appl. Phys. A Mater. Sci. Process. 125, 1 (2019).
[12] R. Ranga, K. Kumar, and A. Kumar, Mater. Chem. Phys. 289, 126482 (2022).
[13] P. Chandra Sati, M. Arora, S. Chauhan, M. Kumar, and S. Chhoker, J. Phys. Chem. Solids 75, 105 (2014).
[14] M. Arora and M. Kumar, Mater. Lett. 137, 285 (2014).
[15] R. Verma, A. Chauhan, Neha, K. M. Batoo, R. Kumar, M. Hadhi, E. H. Raslan, J. Alloys Compd. 21, 116296 (2020).
[16] R. Pandey, C. Panda, P. Kumar, and M. Kar, J. Sol-Gel Sci. Technol. 85, 166 (2018).
[17] C. Fanggao, S. Guilin, F. Kun, Q. Ping, and Z. Qijun, J. Rare Earths 24, 273 (2006).
[18] P. Kumar and M. Kar, Phys. B Condens. Matter 448, 90 (2014).
[19] N. Hernández, V. A. González-González, I. B. Dzul-Bautista, J. Gutiérrez, J. M. Barandiarán, I. Ruiz De Larramendi, R. F. Cienfuegos-Pelaes, and U. Ortiz-Méndez, J. Alloys Compd. 638, 282 (2015).
[20] A. Aharoni, J. Appl. Phys. 56, 3479 (1984).
[21] P. W. Anderson, Phys. Rev. 79, 705 (1950).
[22] R. Ranga, K. Kumar, and A. Kumar, Mater. Chem. Phys. 289, 126482 (2022).
[23] F. Yan, G. Xing, R. Wang, and L. Li, Sci. Rep. 5, 1 (2015).
[24] N. Sheoran, M. Saini, A. Kumar, V. Kumar, T. Kumar, and M. Sheoran, MRS Adv. 4, 1659 (2019).
[25] L. Phor, S. Chahal, and V. Kumar, J. Adv. Ceram. 9, 576 (2020).
[26] M. M. Rhaman, M. A. Matin, M. A. Al Mamun, A. Hussain, M. N. Hossain, B. C. Das,
[27] M. A. Hakim, and M. F. Islam, J. Mater. Sci. Mater. Electron. 31, 8727 (2020).P. Jain, S. Shankar, and O. P. Thakur, Mater. Today Proc. 67, 742 (2022).
[28] T. Sahu and B. Behera, J. Mater. Sci. Mater. Electron. 29, 7412 (2018).
[29] A. K. Sahu, S. K. Satpathy, S. K. Rout, and B. Behera, Trans. Electr. Electron. Mater. 21, 217 (2020).
[30] K. S. Kumar, S. Ramu, A. Sudharani, M. Ramanadha, G. Murali, and R. P. Vijayalakshmi, Phys. E Low-Dimensional Syst. Nanostructures 115, 113689 (2020).
[31] M. Kumar, S. Shankar, O. Parkash, O. P. Thakur, J Mater Sci: Mater Electron 25, 888–896 (2014).
[32] N. Hernández, V. A. González-González, I. B. Dzul-Bautista, J. Gutiérrez, J. M. Barandiarán, Larramendi I. Ruiz De, Cienfuegos-Pelaes R. F., and Ortiz-Méndez U., J. Alloys Compd. 638, 282 (2015).

